Original Article

HUC-MSCs combined with platelet lysate treat diabetic chronic cutaneous ulcers in Bama miniature pig

Yunyi Gao [a, b, c, 1], Lihong Chen [a, b, 1], Yan Li [a, b], Shiyi Sun [a, b], XingWu Ran [a, b, 1, *]

[a] Department of Endocrinology & Metabolism, West China Hospital of Sichuan University, Chengdu, China
[b] Innovation Research Center for Diabetic Foot, Diabetic Foot Care Center, West China Hospital of Sichuan University, Chengdu, China
[c] Department of Medical Affairs, West China Hospital of Sichuan University, Chengdu, China

A B S T R A C T

Human umbilical cord mesenchymal stem cells (HUC-MSCs) and platelet lysate (PL) shows potential of wound healing. However, MSCs in combination with PL for wound healing is still lacking. In this study, we presented high glucose cultured wound related cells to mimic diabetic chronic ulcers (DCU) cells, wound healing indicators and the TGFβ/Smad signaling pathway were detected by PL cultured HUC-MSC supernatant (MSC-Sp) in vitro. In vivo study, diabetes was induced in pigs feeding a high-energy diet and multiple injections of streptozotocin (125 mg/kg). Chronic wounds were created on both sides of the backs of seven pigs by surgical creation and foreign body compression for eight weeks before treatment. The wounds were treated with saline control (N = 11), PL (N = 11), HUC- MSCs (N = 18, 6×10^6/mL/cm^2), and PL + HUC-MSCs (N = 18, 6×10^6/mL/cm^2) respectively. Tissue samples were collected to observe new collagen, neovascularization, wound healing factors, and the TGFβ/Smad signaling pathway. The resulting PL-cultured MSC-Sp promoted the proliferation of keratinocytes, fibroblasts, and vascular endothelial cells and inhibited the TGFβ1/TGFβ3 ratio, upregulated VEGF-α and PDGF-BB production by keratinocytes and fibroblasts, and downregulated the expression of CD86, IL-6, and TNF-α in RAW264.7 cells. PL + HUC-MSCs had the best wound healing rate in vivo, and promoted collagen formation, neovascularization, and inflammation, regulated the balance between IL-6/TGFβ1 and IL-6/Arg-1 and upregulated the expression of VEGF-α and TGFβ1. In summary, PL + HUC-MSCs had a better wound healing effect than HUC-MSCs or PL treatment alone by regulating the IL-6/Arg-1 and IL-6/TGFβ1 balance and upregulating TGFβ1, VEGF-α, Col1, and α-SMA.

© 2024 The Author(s). Published by Elsevier BV on behalf of The Japanese Society for Regenerative Medicine. This is an open access article under the CC BY-NC-ND license (http://creativecommons.org/licenses/by-nc-nd/4.0/).

1. Introduction

Diabetic chronic cutaneous ulcers (DCU) are one of the most common chronic skin ulcers, although there are many measures to treat chronic wounds, such as surgical debridement, negative pressure suction, autologous platelet-rich gels, platelet-derived growth factors, and bioengineered skin [1], their clinical efficacy remains limited. In addition, DCU imposes a high five years

mortality as well as a heavy economic burden on society [2]. Therefore, there is an urgent need to develop novel and effective treatment strategies.

Mesenchymal stem cells (MSCs) are the most mature and widely used stem cells, and human umbilical cord stem cells (HUC-MSCs) were separated from Wharton's Jelly, a colloidal tissue surrounding the umbilical cord blood canal, which is usually discarded during childbirth. Thus, the collection is non-invasive and poses few ethical problems. HUC-MSCs have strong proliferation ability, immunomodulation, and low immunogenicity [3]. HUC-MSCs have been demonstrated to have the potential to promote wound healing by regulating local inflammatory responses [4,5], angiogenesis, granulation tissue formation, collagen remodeling, and epithelization [6—8]. However, the problem is the low proliferation rate of MSCs after transplantation, or massive cell death on the first day after transplantation [9—11]. This may be one of the reasons for the

poor wound healing in some studies [12]. Researchers have found that bio scaffolds improve MSCs survivability and promote wound healing [13]. Platelet lysate (PL) are platelet derivatives obtained by enriching platelets in the blood of volunteers or collecting platelets within 5–7 days without transfusion, through multi-step treatment, and finally fully lysing and activating, releasing platelet particles and various nutrients in the membrane structure [14]. PL is widely used not only in the field of wound repair but also in human cell culture, commercialized PL has been widely used in the production of MSCs [15–17], with potential for translational clinical applications. MSCs combined with PL therapy could improve perfusion of rat hindlimb ischemia [18] and human erectile dysfunction [19], and PL-cultured HUC-MSCs supernatant (MSC-Sp) had a better wound healing promoting effect than fetal bovine serum-supplemented HUC-MSCs supernatant in vitro [20]. These findings suggest that this combination may enhance wound repair. However, there is limited research on wound healing using MSCs in combination with PL therapy.

The wound healing process is divided into hemostasis, inflammation, proliferation, and remodeling phases, and during proliferation phase, M2 macrophages release growth factors, such as vascular endothelial growth factor (VEGF), platelet-derived growth factor (PDGF), and transforming growth factor-beta (TGFβ), which contribute to the shift to the proliferation phase, promote angiogenesis, re-epithelialization, and collagen production [21]. In which, the TGFβ/Small mothers against decapentaplegic (Smad) signaling pathway is the most canonical pathway regulating the formation of collagen in the fibroblasts and myofibroblasts [22]. Researchers have found that HUC-MSCs enhance the local effective distribution and adhesion of wounds by secreting TGFβ1 and improving the long-term survival rate [23]. HUC-MSCs combined with biomaterials also upregulated TGFβ1 expression in wound areas to promote healing [24]. However, exosomes of HUC-MSCs were reported to inhibit dermal fibroblast-myofibroblast conversion by inhibiting the TGFβ/Smad signaling pathway, thereby inhibiting wound fibrosis and scar repair [20]. PL promotes cardiomyocyte differentiation by upregulating myocardial fibroblast TGFβ1 expression [25]. However, research on the application of MSCs in combination with PL for wound healing is still lacking.

Therefore, this study was conducted to evaluate the healing effect of HUC-MSC cultured with PL in stimulating diabetic keratinocyte, vascular endothelial cells and fibroblasts (in vitro study) and on chronic wound healing in diabetes-induced pigs compared to control treatment (in vivo study). We hypothesized that HUC-MSCs combined with PL could promote the cutaneous wound healing process via regulating the TGF-β/Smad signaling pathway.

2. Materials and methods

2.1. Experimental animals, cells, and main reagents

HUC-MSCs at passage three were purchased from Chengdu Konjin Biotechnology Co., LTD (Chengdu, China). Human keratinocytes (HaCat), human dermal fibroblasts (HDF-n), human umbilical vein vascular endothelial cells (HUVEC) were purchased from ScienCell Research Laboratories (California, America). Mouse peritoneal macrophages (RAW264.7) were purchased from Guangzhou Jennio Biotech Co. Ltd. (Guangzhou, China). Streptozotocin (STZ) was purchased from Sigma-Aldrich (St. Louis, Missouri, USA).

PL was purchased from Biological Industries (Beit-Haemek, Israel). Anti-CD14, human leukocyte antigen DR (HLA-DR), anti-CD34, anti-CD44, anti-CD75, and anti-CD103 antibodies were purchased from Cyagen (Suzhou, China). TRIzol reagent kits were purchased from Invitrogen (Thermo Fisher Scientific). VEGF-α, PDGF-BB, and TGFβ1 enzyme-linked immunosorbent assay (ELISA)

kits were obtained from R&D Systems (Minneapolis, MN, USA). TGFβ1 polyclonal Antibody, SMAD7, and TGFβ3 polyclonal antibody were purchased from Proteintech (Abcam, Cambridge, United Kingdom). Smad3 (C67H9) rabbit mAb, Phospho-Smad3 Rabbit mAb, Smad2/3 Rabbit mAb, and Phospho- Smad2/Smad3 Rabbit mAb were purchased from Cell Signaling Technology (Danvers, MA, USA). Mouse anti-GAPDH mAb was purchased from BioX (Belgium; New Hampshire, USA).

2.2. HUC-MSCs identification and supernatant collection

Passages 3 generation HUC-MSCs were cultured in α-MEM basal medium with 5 % PL in a 37 °C incubator with 5 % CO2 in a 95 % humidified atmosphere, and replaced every three days. PL-cultured P5 cells were tested for phenotypes using fluorescence-cultured cell sorting (FACS) analysis. The antibodies used were anti-CD14, HLA-DR, anti-CD34, anti-CD44, anti-CD73, and anti-CD105 antibodies. P4 HUC-MSC differentiation into osteogenic and adipogenic lineages and subsequent detection was performed using established methods [7]. Control cells were treated with the standard culture medium for 14 days. P5 and P6 HUC-MSCs were inoculated in a 15 cm Petri dish. When the cells reached 80 % confluence, serum-free α-MEM was added to the dish, and MSC-Sp was collected after 48 h. The liquid was centrifuged at 4 °C, 12000 g for 15 min after 0.22 μm filter filtration retention supernatant, frozen at −80 °C for detection and experimentation.

2.3. HUC-MSCs intervention diabetic wound related cell models

HaCat, HDF-n, and HUVEC were passaged in high glucose (25 mmol/L) [25,26] medium containing 10%FBS to mimic diabetic ulcer-related cells and then treated with MSC-Sp for subsequent experiments considering the paracrine effect of HUC-MSCs. In addition, hyperglycemic pre-cultured RAW264.7 cells were used to evaluate the effects of MSC-Sp on inflammation.

2.4. CCK8 cell proliferation assays

Hyperglycemic passaged HaCat, HDF-n, and HUVEC were seeded in 96-well plates (1×10^5 cells/well). After adhering to the walls, they were treated with MSC-Sp and observed for 24 h, 48 h and 72 h. The cells were then incubated with 10 μL of CCK-8 reagent (Dojindo, Kumamoto, Japan) for 4 h after treatment with MSC-Sp every 24 h group. Control cells were treated with PL-free culture medium simultaneously. Absorbance was measured data wavelength of 450 nm. The faster the cell proliferation, the darker the color and the greater the absorbance values.

2.5. Cell proliferation gene expression with RT-qPCR

Cell proliferative cyclin gene expression (including Cyclin D2, Cyclin A1 and C-Myc) was detected by RT-qPCR. A TRIzol reagent kit was used for RNA extraction. The isolated RNA was reverse-transcribed into complementary DNA using the PrimeScript RT Kit (TaKaRa, Japan). Primers were synthesized by Tsingke Biotechnology Co., Ltd. (Beijing, China), and are listed in Supplemental Table 1. PCR was performed on a Roche Real-Time System (Roche, Basel, Switzerland) using a SYBR1 Premix Ex *Taq*II kit (TaKaRa, Japan). Controls cultured in PL-free medium were used to calculate relative gene expression using ΔΔct and $2^{-\Delta\Delta ct}$.

2.6. In vitro wound healing experiment

Hyperglycemic passaged HaCat, HDF-n, HUVEC cells (1×10^5 cells per well) were seeded in six-well plates and when

they reached 90 % confluence, they were scratched using a standard 200 μL pipette tip. Cells within the wound area were washed with PBS and treated with 2 mL α-MEM culture medium without serum or PL (control group). Three other wells were treated with 2 mL PL-free MSC-Sp. All plates were incubated at 37 °C in 5 % CO_2 for 48 h and media wound not change during this period. Three photomicrographs of each scratch were obtained at the initial time of wound creation, and the same location was photographed every 12 h until completion of the study. The ImageJ Software (National Institutes of Health, NIH, USA) was used to quantify the remaining area of the wound. After completion of each scratch assay, 1 mL MSC-Sp was stored at −80 °C until ready for analysis. The concentrations of VEGF-α, PDGF-BB, and TGFβ1 were measured using human ELISA kits. The control group contained α-MEM and MSC-Sp. These wound-healing factors were also detected by RT-qPCR, and the primers used are listed in Supplemental Table 1.

2.7. In vivo diabetic chronic wound construction

Bama miniature pigs were purchased from Chengdu Dossy Experimental Animals Co. Ltd (Chengdu, China). Five pigs (named D1, D2, D3, D4, and D5) were fed a high-energy diet from 19 weeks of age as the diabetic group, and the other two pigs were fed a control diet as non-diabetics (C1 and C2). Diabetes was induced by a high-energy diet combined with an intravenous injection of STZ (125 mg/kg), and the average fasting blood glucose level of diabetic pigs was higher than 7 mmol/L, which was considered a successful model [27]. For wounding, pigs (61.8 ± 8.0 kg, average body length 98.9 ± 4.2 cm) were anesthetized with atropine sulfate (0.05 mg/kg, CR Double Crane, China) and Soletil 50 (4 mg/kg, Virbac, France) after fast for 8 h. Isoflurane (Merck, USA) was used to maintain anesthesia. To avoid the bone and joint, the average body length was 50.1 ± 3.4 cm, which suitable for wounding. Full-thickness cutaneous ulcers of 3 cm in diameter and spaced at least 3 cm apart was surgically created on both sides of the spine, and there were 5 or 6 wounds per side along the spine. Wounds were then filled with self-designed foreign material to help inhibiting wound healing thus building a chronic cutaneous ulcer model (Supplemental Fig. 1). And there were 20 wounds in non-diabetic pigs and 58 wounds in diabetic pigs. Dressings were changed every six days, and wounds were sectioned for histology and assessment of inflammatory indicators for eight weeks, in which specimens collected at the time of wounding were used as pre-wound normal tissue controls. Wounds cannot heal through the normal healing process [28] and do not heal for at least eight weeks, indicating a successful chronic cutaneous wound model.

2.8. Treatment and wound healing assessment

Chronic wound models were successfully created and randomly divided into a non-diabetic normal saline treatment group (NDM-NS, pigs = 2, n = 10) and a non-diabetic PL treatment group (NDM-PL, pigs = 2, n = 10). The wounds of the diabetic pigs were assigned to the normal saline treatment group (DM-NS, pigs = 2, n = 11), PL treatment group (DM-PL, pigs = 2, n = 11), HUC-MSCs treatment group (DM-MSCs, pigs = 2, n = 18), and PL + HUC-MSCs treatment group (DM-PL + MSCs, pigs = 2, n = 18) (Supplemental Fig. 2). The HUC-MSCs of the P4–P6 generation were dissolved in normal saline and PL solution at 6×10^6/mL and treated as 6×10^6/mL/cm^2 by multiple injections in the wounds, consistent with other large animal model studies [29–31] and our per-experimental effects. The NDM-NS and NDM-PL groups were treated with equal wound volumes. Dressing changes were performed every three days after treatment. On the third, sixth, ninth, and the twelfth days, wounds were traced and photographed. Wound area was calculated by

using the method of "Wound Edge Mapping + Digital Photography + ImageJ Software ". Healing rate = [(initial area of wound-unhealed area)/initial area of wound] × 100 % [32].

2.9. Tissue specimen collection and histology examination

To minimize the impact on wound healing, wound areas within the range of normal to granulation tissue were collected under local anesthesia with 2 % lidocaine (approximately 1–2 mm were collected at five different time points: before treatment (D0), 3 days (D3), 6 days (D6), 9 days (D9), and 12 days (D12)) alternately every three days in each treatment group by a biopsy device, and ensuring a minimum of 6 samples in each group. HE staining was used to evaluate the inflammation status, wound repair indicators. Masson's trichrome staining was used to observe new collagen. The integrated optical density (IOD) and area of all acquired images were determined using Image-Pro Plus 6.0 image analysis system, and the percentage of collagen tissue expression area was calculated. CD31 (Abcam, Cambridge, Britain, ab28364, 1:50) staining was used to observe the micro vessel density (MVD) following the general immunohistochemistry protocol.

2.10. Wound healing factors and inflammatory factors evaluation

In vitro experiment, interleukin 6 (IL-6) and tumor necrosis factor α (TNF-α) were detected by RT-qPCR in hyperglycemic cultured RAW264.7 cells and after treated by MSC-Sp. VEGF-α and PDGF-BB in HaCat, HDF-n, and HUVEC treated with MSC-Sp were tested by Rt-qPCR and ELISA, and the controls were treated with the control medium. The mouse-specific primers are listed in Supplemental Table 2. For the in vivo experiment, wound samples were collected during the chronic wound modeling period (including pre-wound (D0), wound 6 days (wound 6D), wound 24 days (wound 24D), and wound 56 days (wound 56D)) and after treatment D0, D3, D6, D9, and D12. Rt-qPCR was performed to assess the expression of IL-6, TNF-α, VEGF-α, PDGF-BB, alpha-smooth muscle actin (α-SMA), and collagen types I and III (Col1 and Col3). The reverse-transcription primers used are listed in Supplemental Table 3. Pre-wound and D0 samples were used as controls to calculate relative mRNA expression according to the manufacturer's protocol.

2.11. TGFβ/Smad signaling pathway expression analysis

TGFβ/Smad signaling pathway expression was assessed in both in vivo and in vitro wounds by RT-qPCR and western blotting. For western blotting, the cells or tissues were homogenized in RIPA buffer and mixed on ice for 30 min. Lysates were centrifuged at 12,000×g for 30 min at 4 °C and the supernatant was collected. The protein concentration in the supernatant was determined using a bicinchoninic acid assay. Equal amounts of protein (20 μg) were separated by 10%SDS-PAGE and transferred to a polyvinylidene difluoride membrane. Membranes were blocked with 3 % BSA in TBST for 1 h and incubated with primary antibodies overnight at 4 °C, then washed with TBST, and developed using an alkaline phosphatase color development kit. The bands were visualized using an enhanced chemiluminescence kit. Images were captured using ChemiDoc™(BioRad) with Image Lab software, and the densities of the blots were quantified using the Quantity One analysis software. Supernatants were analyzed using a bicinchoninic acid assay. Equal amounts of protein (20 μg) were separated by 10 % SDS-PAGE and transferred to a polyvinylidene difluoride membrane. Membranes were blocked with 3 % BSA in TBST for 1 h and incubated with primary antibodies overnight at 4 °C, then washed with TBST, and developed using an alkaline phosphatase

color development kit. The bands were visualized using an enhanced chemiluminescence kit. Images were captured using ChemiDoc™(BioRad) with Image Lab software, and the densities of the blots were quantified using the Quantity One analysis software.

2.12. Statistical analysis

SPSS 22.0 was used for statistical analysis. If the quantitative data conformed to the normal distribution, the data were expressed as mean $\pm$ standard deviation (SD) (mean $\pm$ SD). Normality and homogeneity of variance tests were performed. We used an independent samples t-test and one-way analysis of variance (ANOVA) to compare the means of different groups, and the Scheffe post-hoc test was used to analyze differences between groups. Two-way repeated-measures ANOVA was used to analyze the data at multiple time points between the groups. After the data were subjected to Mauchly's Test of Sphericity, those that did not meet the sphericity test were corrected using the Greenhouse-Geisser (G-G) method. If there was a difference between the groups, the Scheffe post hoc test was used when the sample size of each group was different, and Tamhane 2 analysis was used when the variance was uneven. $P \leq 0.05$. GraphPad Prism, Adobe Illustrator, and Adobe Photoshop software were used to complete the charts in this study.

3. Results

3.1. HUC-MSCs identification

P5 HUC-MSCs were positive for MSCs markers, such as CD44, CD105, and CD73, and negative for hematopoietic markers, such as CD14, CD34, and HLA-DR (Supplemental Fig. 3), using a Flow Cytometer. MSCs subjected to osteogenic and adipogenic culture conditions differentiate into osteocytes and adipocytes, respectively. Oil Red O staining showed lipid vacuoles stained red, whereas Alizarin Red S staining showed deposits of calcium crystals stained orange to brown (Supplemental Fig. 3), confirming their identity as MSCs according to the accepted criteria [33].

3.2. PL-cultured MSC-Sp promoted diabetic ulcer-related cells healing

Compared with α-MEM basal medium, PL-cultured MSC-Sp significantly promoted the proliferation and healing rates of HaCat, HDF-n, and HUVEC. At time points 24 h, 48 h, and 72 h post- CCK8 staining, the MSC-Sp group had significantly increased cell proliferation rates of HaCat, HDF-n, and HUVEC ($p < 0.01$.) (Fig. 1A–C). Cyclin D2, Cyclin A1, and C-Myc expression levels in HaCat cells were significantly elevated (p values were all less than 0.05). Cyclin A1 of HDF-n was elevated significantly ($p = 0.012$), and Cyclin D2 and C-Myc gene expression in HUVEC was elevated significantly (p values were all less than 0.05), after treatment with MSC-Sp (Fig. 1D–F). At time points 12 h, 24 h for HaCat, 24 h for HDF-n, 48 h for HUVEC after the scratch assay, the MSC-Sp group showed a significant increase in wound closure rate compared to the control group (p values were less than 0.01.) (Fig. 1G–I).

3.3. MSC-Sp promoted diabetic ulcer-related cells secreting VEGF-α, PDGF-BB

Except VEGF-α or PDGF-BB, only TGFβ1 was detected in MSC-Sp, with an average concentration of 98.070 ± 2.700 pg/ml before
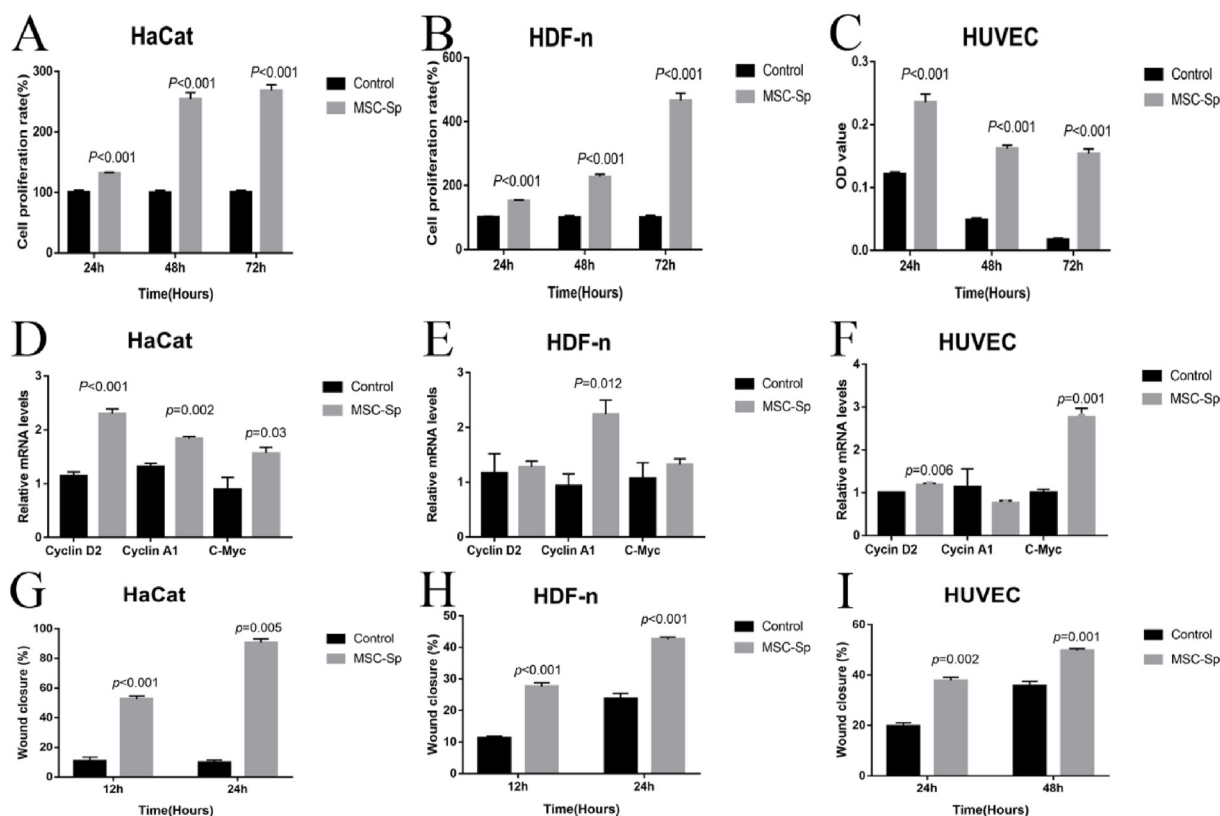

Fig. 1. MSC-Sp promoted diabetic ulcer-related cells proliferation and migration
A), B) and **C)**, CCK8 experiment, n = 6,13 and 9 of HaCat , HDF-n and HUVEC respectively , CCK8 results of HUVEC was OD value for the data was not suitable for proliferation rate. **D), E)** and **F)**, QPCR results of proliferative cyclin, n = 5,4 and 4 of HaCat, HDF-n and HUVEC respectively. **G), H)** and **I)**, Scratch test, n = 3,7 and 4 of HaCat, HDF-n and HUVEC respectively.

Table 1
Growth factors levels before and after MSC-Sp treatment.

Growth factors	MSC-Sp VS. Control (n = 3)	MSC-Sp VS. Control, after treatment for 48 h (n = 3)		
		HaCat	HDF-n	HUVEC
TGFβ1(pg/mL)	98.070 VS. 0	0 VS. 0	0 VS. 0	0 VS. 0
VEGF-α(pg/mL)	0 VS. 0	8494.510 VS. 520.520	1296.162 VS. 0	0 VS. 0
PDGF-BB(pg/mL)	0 VS. 0	133.990 VS. 20.810	0 VS. 0	0 VS. 0

treatment. However, none of them secreted TGFβ1 after treatment of HaCat, HDF-n, or HUVEC with MSC-Sp (Table 1). HaCat secreted VEGF-α and PDGF-BB in both control medium and MSC-Sp. However, MSC-Sp significantly promoted secretion of VEGF-α (8494.510 pg/ml vs. 520.520 pg/ml) and PDGF-BB (133.990 pg/ml vs. 20.810 pg/ml) by keratinocytes. MSC-Sp promoted HDF-n secretion of VEGF-α, but it did not promote HUVEC secrete VEGF-α (Table 1). In addition, HDF-n and HUVEC could not secrete PDGF-BB regardless of treatment with MSC-Sp or not in this study. Consistent with ELISA results, MSC-Sp inhibited TGFβ1 expression of diabetic ulcer-related cells compared with control groups, in which the expression of TGFβ1 in HaCat and HDF-n decreased significantly ($p < 0.05$). MSC-Sp significantly promoted VEGF-α and PDGF-BB expression in HaCat and HDF-n (p-values were both less than 0.05), with no upregulation in HUVEC (Fig. 2).

3.4. Successfully construction of diabetic chronic wound

The high-energy diet combined with STZ injection successfully generated a stable pig diabetes model at 76 weeks of age when the diabetes models were built for 29 weeks. The fasting blood glucose (FBG) levels of D1, D2, and D4 were higher than 20 mmol/L and required insulin treatment to avoid ketoacidosis, consistent with the other two pigs, whose OGTT results met the diagnostic criteria compared to non-diabetic pigs (Supplemental Fig. 4).

The wounds did not heal for 56 days (8 weeks) and presented a persistent inflammatory state (Supplemental Fig. 5). As there was a significantly higher expression of IL-6 and TNF-α over time compared with pre-wound tissues, p values were all less than 0.05. The relative expressions of IL-6 and TNF-α were 15.627 ± 2.834 and 9.220 ± 2.089, respectively, at 56 days. In the in vitro experiment, hyperglycemic medium also increased the expression of CD86, IL-6, and TNF-α compared to normal glucose medium ($p < 0.05$, Fig. 3).

3.5. HUC-MSCs and PL promoted wound healing

NDM-PL had significantly higher wound healing rates at all time points than the DM-PL, NDM-NS, and DM-NS groups (p < 0.05), suggesting that diabetes delayed wound healing, whereas PL promoted it (Supplemental Tables 4 and 5 and Fig. 4). HUC-MSCs, PL, and PL + HUC-MSCs treatment significantly promoted wound healing compared to NS (p values were all less than 0.05), in which PL + HUC-MSCs treatment had the best wound healing rate. Typically, on day 12, the average wound healing rates were 67.362 ± 6.368 % in DM-NS group, 75.791 ± 2.885 % in DM-PL group, 73.509 ± 1.209 % in DM-MSC group, and 83.118 ± 2.765 % in DM-PL + MSCs group, respectively (Supplemental Tables 4 and 5 and Fig. 4). The PL + HUC-MSCs treatment group also showed the greatest effects on dermal maturity, collagen formation, and micro vessel density. Briefly, the PL + HUC-MSCs group had a higher collagen
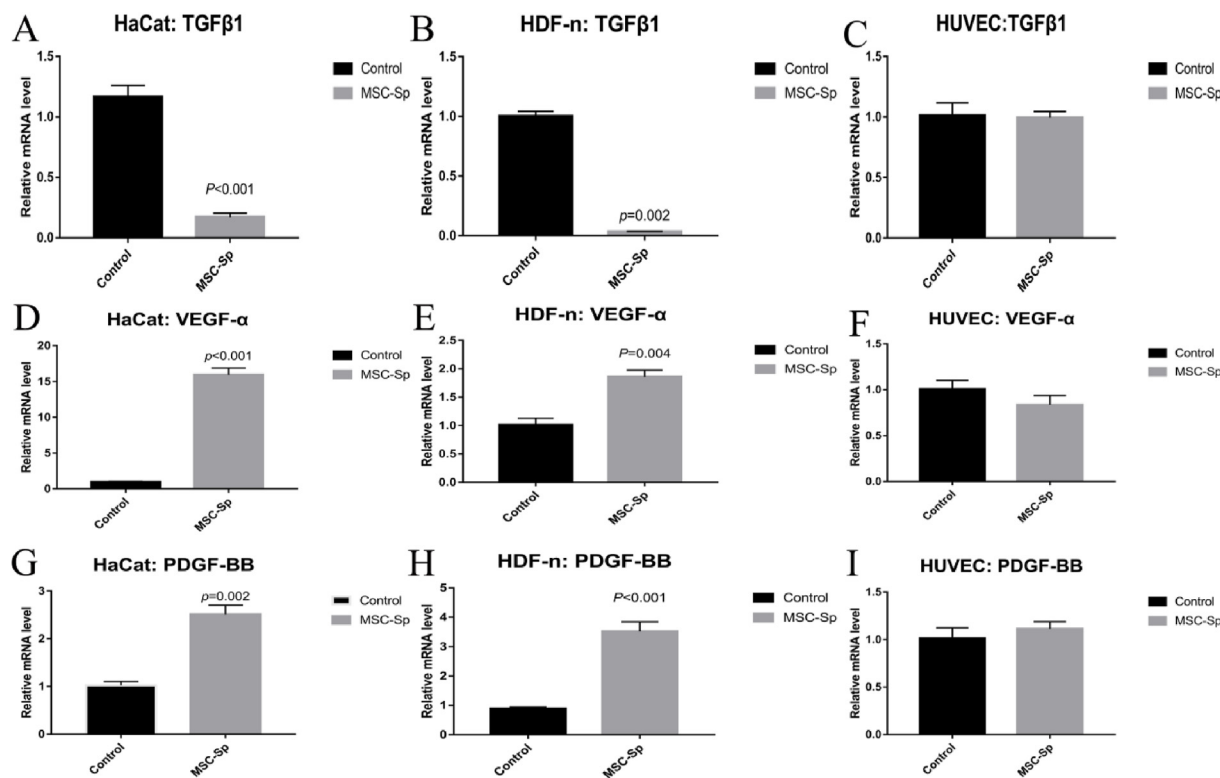

Fig. 2. Relative mRNA levels of growth factors in MSC-Sp after intervention with diabetic ulcer-related cells
A), D) and **G)**: TGFβ1, VEGF-α and PDGF-BB expression in HaCat, n = 4; **B), E)** and **H)**: TGFβ1, VEGF-α and PDGF-BB expression in HDF-n, n = 5; **C), F)** and **I)**: TGFβ1, VEGF-α and PDGF-BB expression in HUVEC, n = 3.
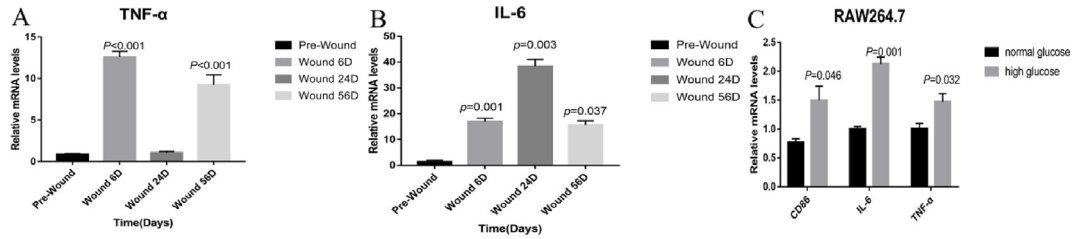
Fig. 3. Inflammatory factors change of in vivo and in vitro modeling
A), TNF-α of DCU modeling period. **B)**, IL-6 of DCU modeling period. **C)**, Expression of CD86, IL-6 and TNF-α expression in high glucose induced macrophages.

concentration than the PL and NS treatment groups ($P < 0.05$, Fig. 5). This was consistent with the higher expression of Col1 and Col3 in the PL + HUC-MSCs group than in the NS group by further exanimating gene expression ($P < 0.05$; Fig. 5). HUC- MSCs tended to have fewer scarring effects, and the relative expression of α-SMA in PL + HUC-MSCs and HUC-MSCs treatment alone was significantly lower than that in the PL and NS treatment groups ($P < 0.001$). The MVD of the PL + HUC-MSCs and HUC-MSCs treatment groups was significantly higher than that of the NS treatment group ($P < 0.05$). In PL + HUC-MSCs group, the relative expression of VEGF-α was also significantly higher than that in NS and HUC-MSCs groups ($P < 0.05$). There was no significant upregulation in PDGF-BB expression among the groups, except for the PL and NS treatments (Fig. 6).

3.6. HUC-MSCs and PL regulated wound inflammation

In the in vitro experiment, MSC-Sp treatment significantly reduced the relative expression of IL-6 and TNF-α compared to the control treatment ($P < 0.001$) in macrophages (Fig. 7A). In the in vivo experiment, during wound healing, the infiltration of inflammatory cells in each group was mainly lymphocytes and

plasma cells, and there were no significant pathological differences among groups, regardless of diabetes status or not. HUC-MSCs significantly reduced IL-6 expression compared to other groups ($P < 0.05$), PL + HUC-MSCs significantly increased Arg-1 and TGFβ1 expression compared to HUC-MSCs alone ($P < 0.05$). Further analysis of the relative expression ratios of IL-6/Arg-1 and IL- 6/TGFβ1 showed no significant difference in IL-6/Arg-1. On the 3rd day after treatment, IL-6/Arg-1 in the PL + HUC-MSCs group was significantly higher than that in the HUC-MSCs group ($P = 0.037$), whereas the IL-6/TGFβ1 ratio was not statistically different between the groups (Fig. 7).

3.7. HUC-MSCs and PL regulated wound TGFβ/Smad signaling pathway

We investigated the underlying mechanism of HUC-MSCs and PL-induced wound healing in affected tissues. The expression level TGFβ1, TGFβ3, Smad2, Smad3, Smad4, and Smad7 were analyzed using western blotting and RT-qPCR. In vitro experiments, the relative gene expression of TGFβ1, Smad2, Smad3, and Smad4 in diabetic ulcer-related cells after PL-cultured MSC-Sp intervention was reduced, while the expression of Smad7 and TGFβ3 was
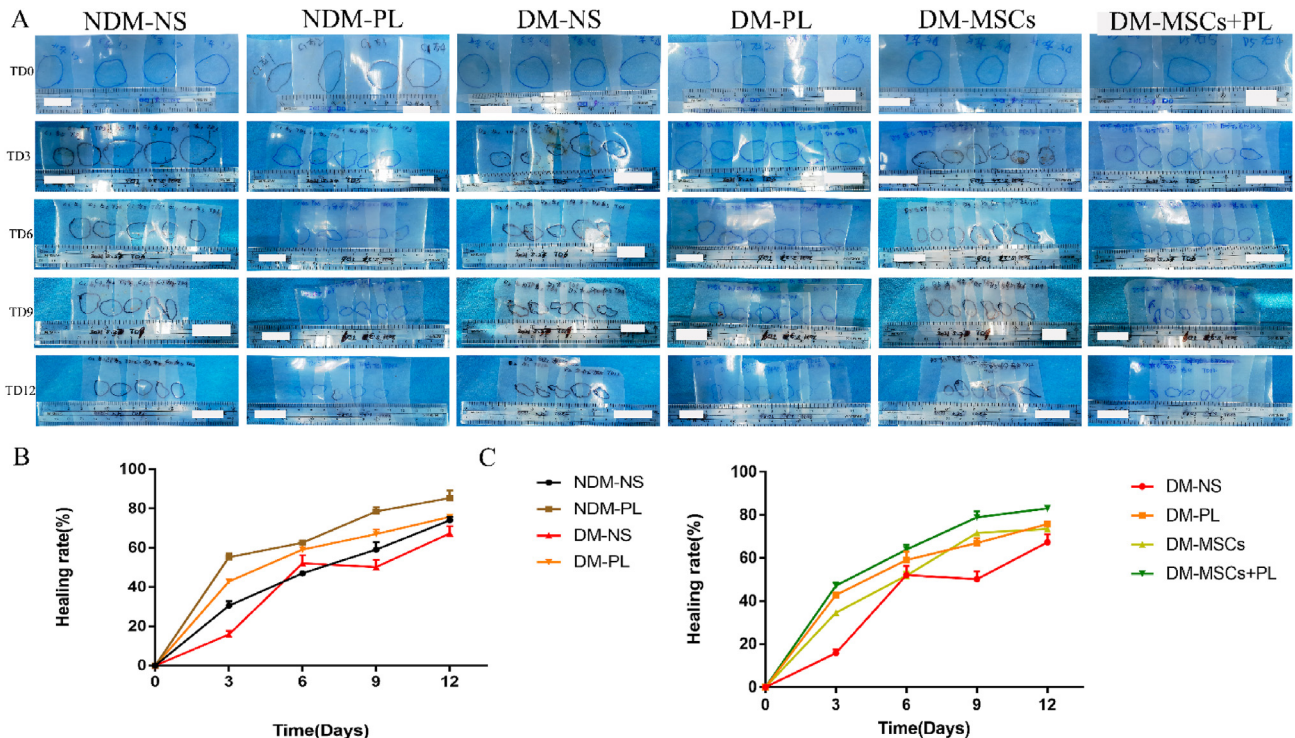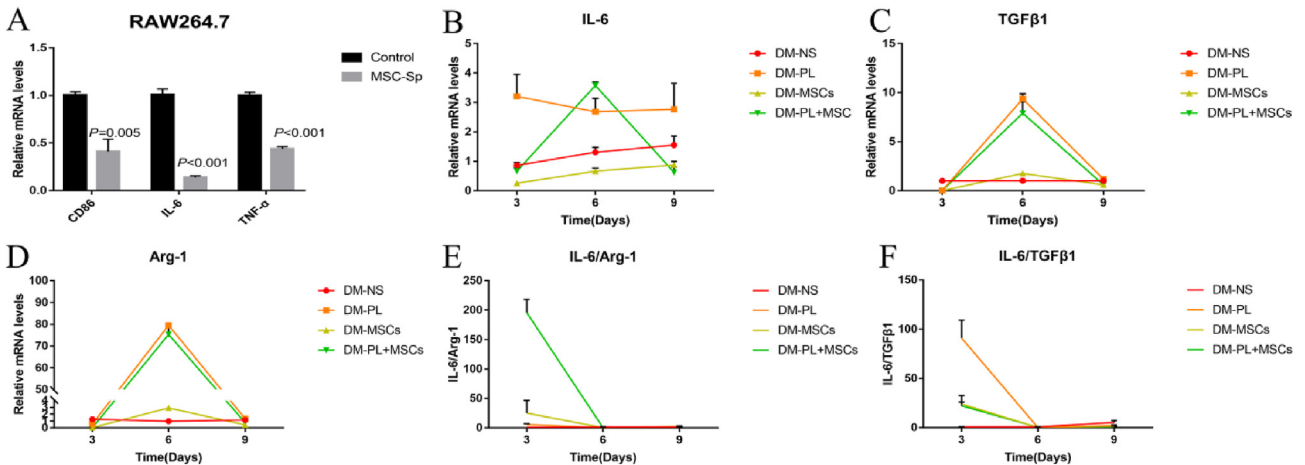

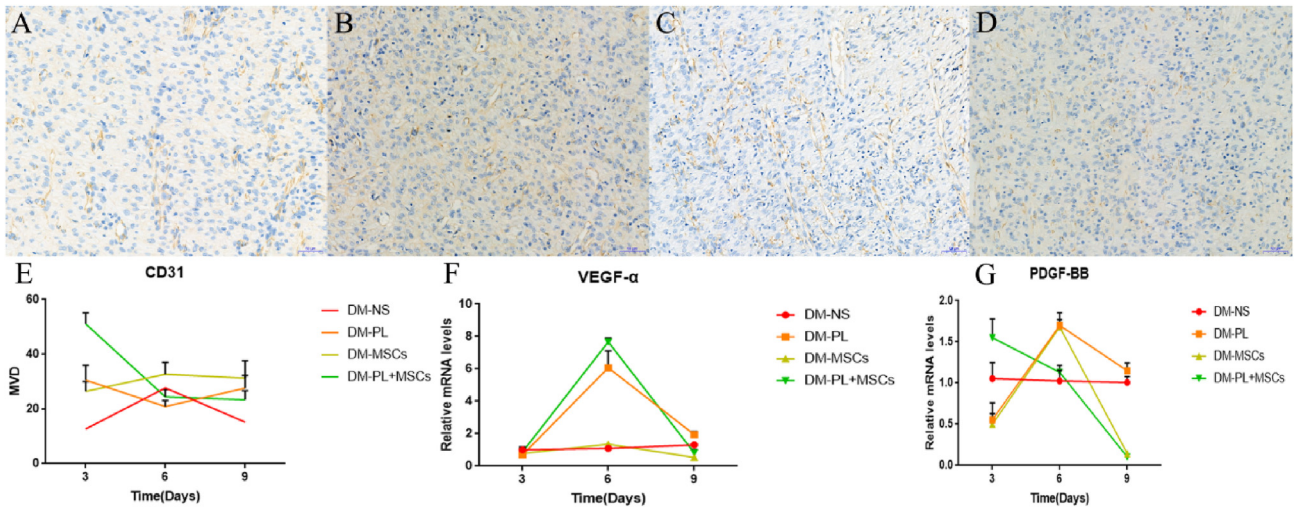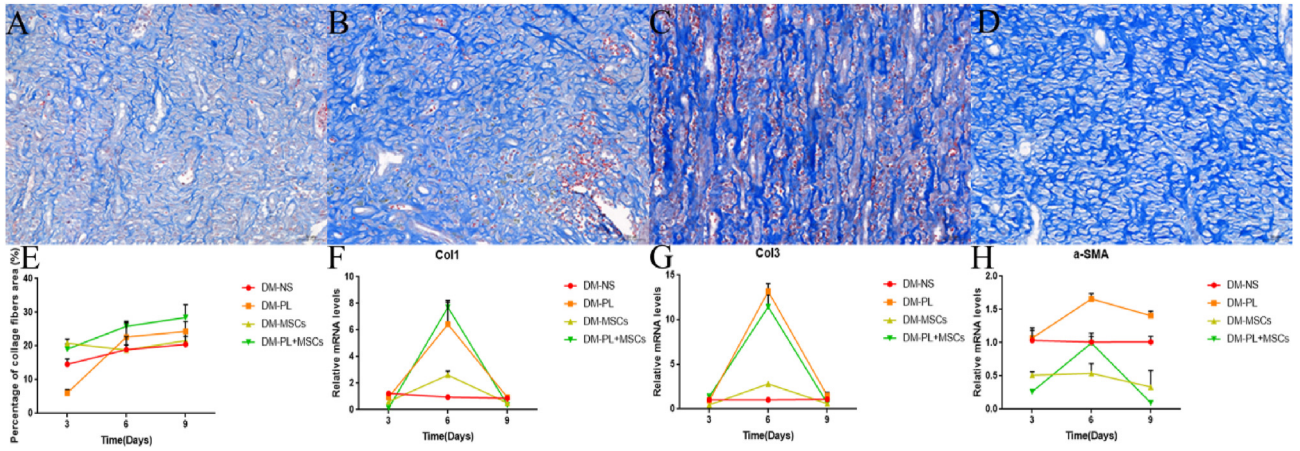
Fig. 4. Wound healing rate in the control and DCU groups
A), Representative figures of wounds area changes of pigs among groups over time. **B)** and **C)**, Wound healing rate in Control and experimental treatment groups respectively.

Fig. 5. Collagen fiber production and related gene expression
A) to **D)** showed representative figures are from 9th day after treatment of Masson's trichrome staining in NS, PL, HUC-MSCs and PL + HUC-MSCs treatment groups respectively (40X). **E)**, the percentage of collage fiber area at each time point of DCU treatment (n = 3). Expression of collagen fiber production factors and DM-NS was control in **F)**, **G)** and **H)**, n = 3.

Fig. 6. MVD production and related gene expression
A) to **D)** showed representative figures are from 9th day after treatment of CD31 immunohistochemical staining in (20X) NS, PL, HUC-MSCs and PL + HUC-MSCs treatment groups respectively. **E)**, The MVD at each time point of DCU treatment (n = 6). **F)** and **G)** Expression of VEGF-α, PDGF-BB in DCU treatment group, DM-NS was control, n = 3.

Fig. 7. Expression of pro-inflammatory factors of in vivo and in vitro experiments
Relative mRNA levels of pro-inflammatory factors in MSC-Sp in macrophages (n = 7). Pro-inflammatory factors expression levels in DCU treatment groups, DM-NS was control and n = 3.

elevated. MSC-Sp also reduced the TGFβ1/TGFβ3 ratio in these cells ($P < 0.05$) (Fig. 8). The protein expression ratio of TGFβ1/TGFβ3 was also reduced in these cells. However, only the difference in HaCat expression was statistically significant ($P < 0.001$) (Fig. 9). In vivo experiments, the relative genes expression of TGFβ1, Smad2, Smad3 and Smad4 in PL + HUC-MSCs and PL treatment groups were significantly higher than that in HUC-MSCs group ($P < 0.05$). Smad7

and TGFβ3 levels were significantly decreased ($P < 0.05$). Thus, the relative ratio of TGFβ1/TGFβ3 in the PL + HUC-MSCs and PL treatment groups was also significantly higher than that in the HUC-MSCs treatment group ($P < 0.05$) (Figs. 7 and 10). The changes in the TGFβ/Smad signaling pathway at day nine were generally consistent among groups, which might be related to the disappear of topical treatment fluids. Thus, we only tested protein expression
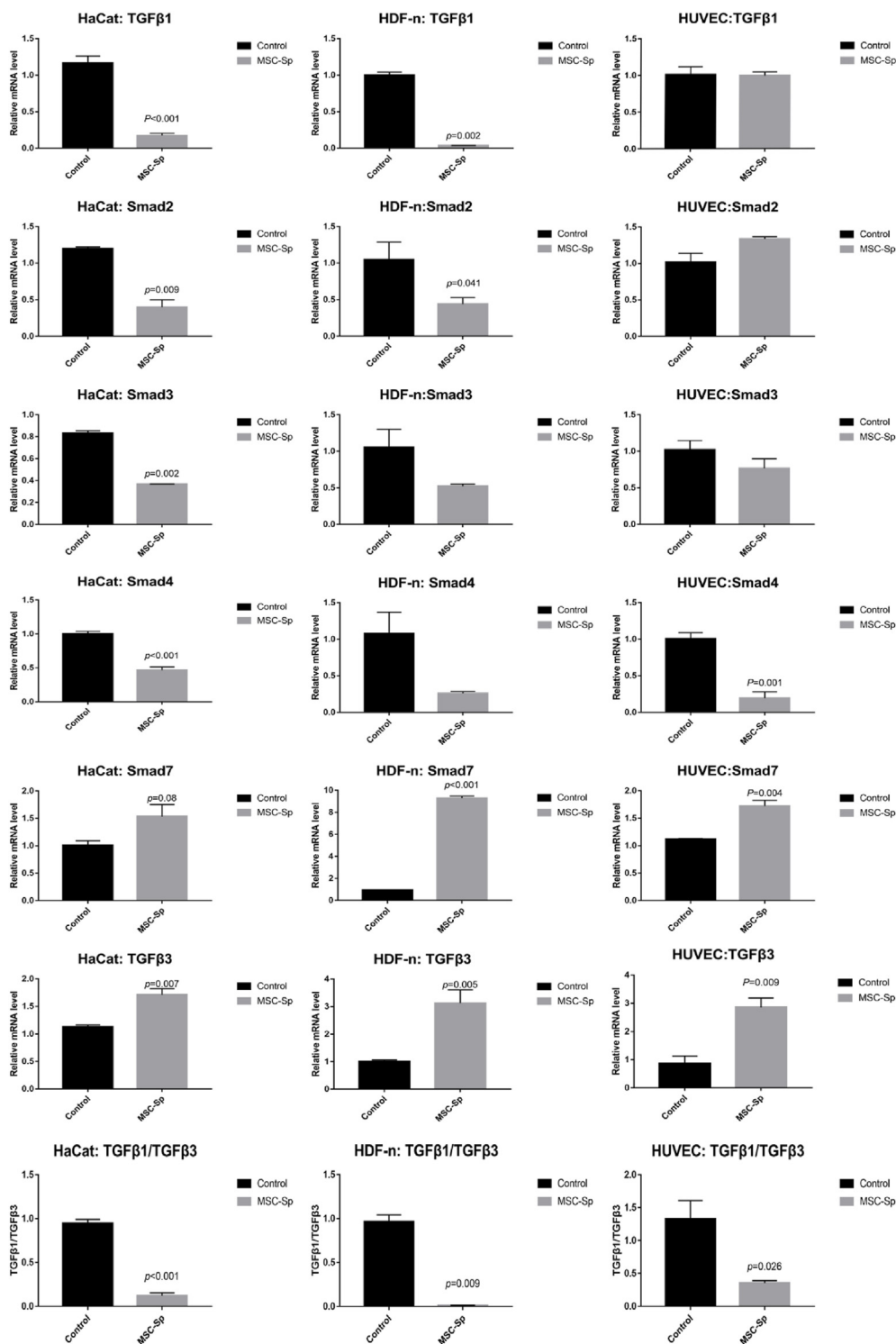

Fig. 8. Expression of TGFβ/Smad signaling pathway of diabetic wound related cells
Relative gene levels of TGFβ/Smad signaling pathway after the intervention by MSC-Sp and control medium of HaCat (n = 3), HDF-n (n = 4) and HUVEC (n = 4).
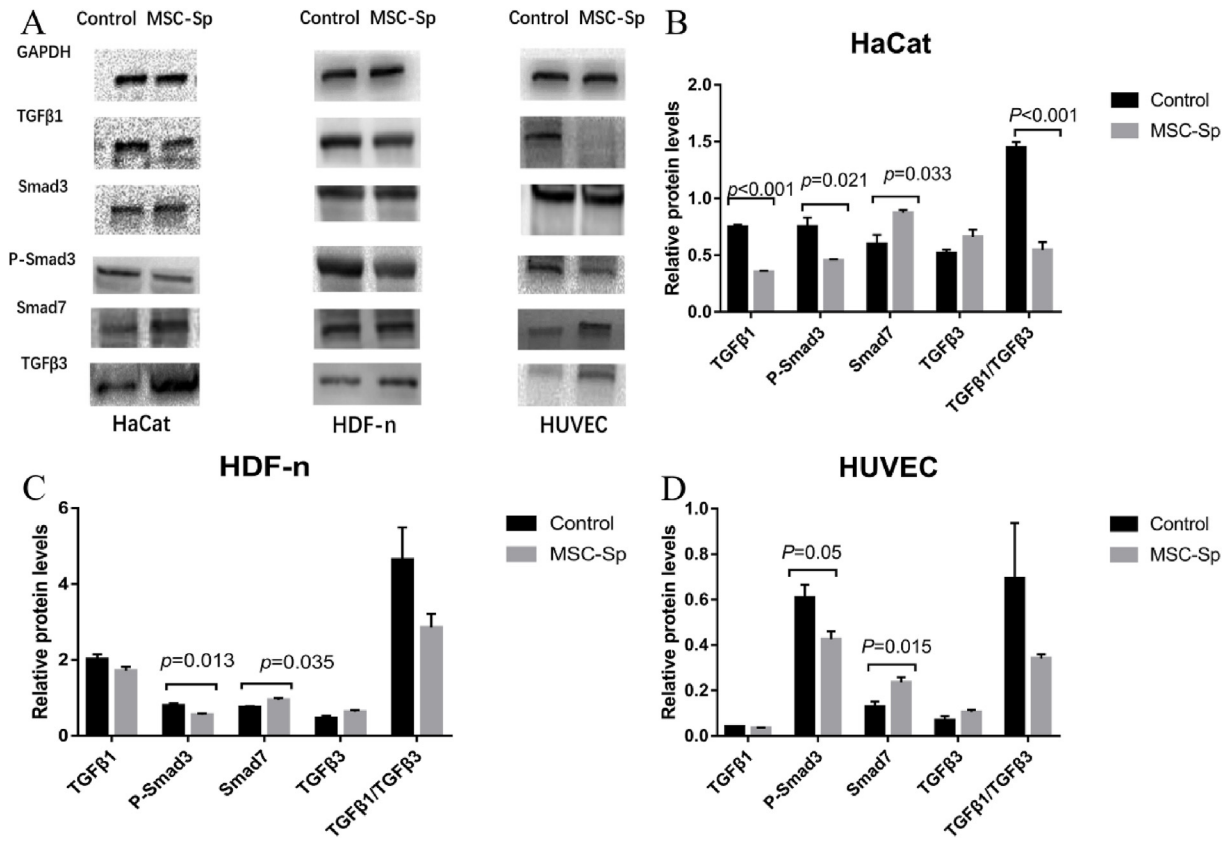
Fig. 9. Expression of TGFβ/Smad signaling pathway of diabetic wound related cells
A), representative WB images of MSC-Sp inhibits diabetic wound repair cells TGFβ/Smad signaling pathway. **B**), **C**), **D**), Relative protein levels of TGFβ/Smad signaling pathway after the intervention by MSC-Sp and control medium of HaCat (n = 3), HDF-n (n = 4) and HUVEC (n = 4). P-Smad3 was the result of P-Smad3/Smad3, and other indicators' results were Indexs/GAPDH.

in wound areas six days after treatment by western blotting. Only TGFβ1, Smad7 and TGFβ3 had significant difference among groups ($P < 0.05$). Consistent with the Rt-qPCR results, the protein ratio of TGFβ1/TGFβ3 in the PL + HUC-MSCs and PL treatment groups was significantly higher than that in the HUC-MSCs group ($P < 0.05$) (Fig. 11). Smad7 expression was significantly higher in the HUC-MSCs group than in the other treatment groups ($P < 0.05$). In summary, PL + HUC- MSCs and PL treatment upregulated the

TGFβ1/TGFβ3 ratio. HUC-MSCs downregulated TGFβ1, Smad2, Smad3, and Smad4, and upregulated genes expression of Smad7 and TGFβ3.

4. Discussion

This study indicated that HUC-MSCs and PL stimulated DCU healing both in vitro and in vivo. PL-cultured MSC-Sp effectively
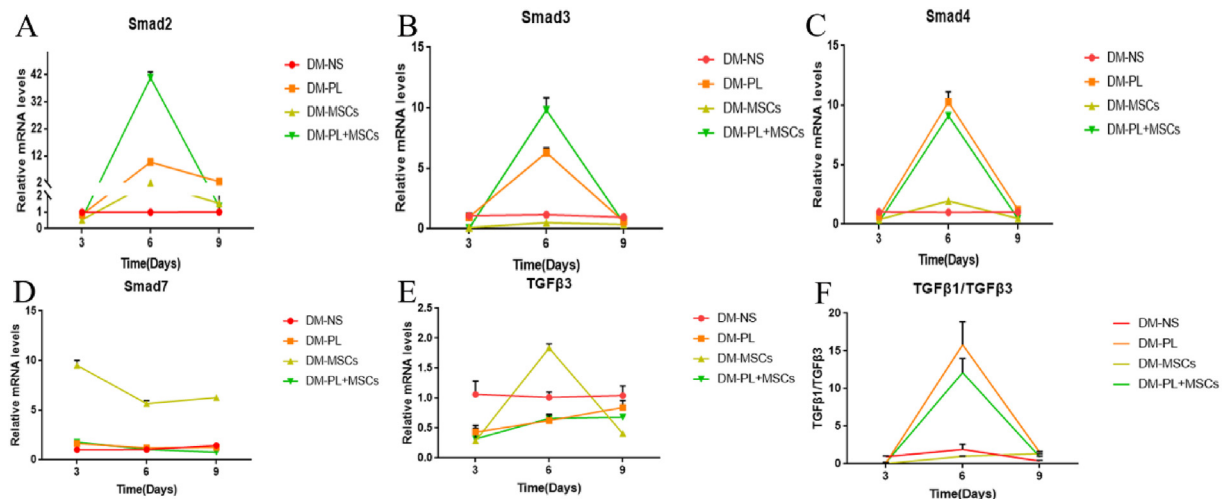

Fig. 10. Relative mRNA levels of TGFβ/Smad signaling pathway in DCU treatment groups
A), Smad2. **B**), Smad3. **C**), Smad4. **D**), Smad7. **E**), TGFβ3. **F**), TGFβ1/TGFβ3, n = 4.
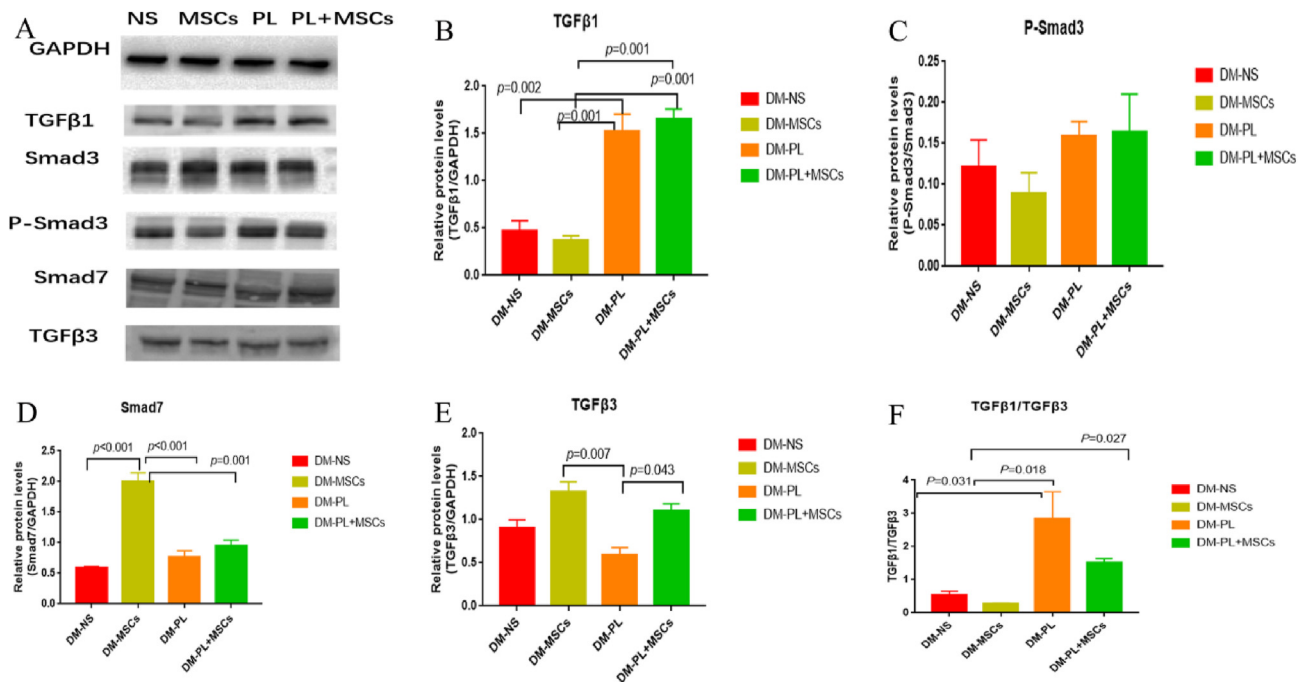
Fig. 11. Expression of TGFβ/Smad signaling pathway of DCU treatment groups
A), representative WB images of TGFβ/Smad signaling pathway in DCU treatment groups at day 6. **B)**, **C)**, **D)** and **E)**, Relative TGFβ1, P-Smad3, Smad7 and TGFβ3 protein levels of TGFβ/Smad signaling pathway after the intervention by DCU treatment groups, n = 4.

promoted diabetic ulcer-related cell proliferation and migration in vitro. HUC-MSCs combined with PL had a synergistic effect on wound healing by regulating the TGFβ/Smad signaling pathway in vivo.

In vitro experiments demonstrated that HUC-MSCs promoted angiogenesis and collagen formation and inhibited scarring via inhibition of the TGFβ/Smad signaling pathway, manifested as an inhibited TGFβ1/TGFβ3 ratio, and promoted VEGF-α and PDGF-BB. MSC-Sp inhibited TGFβ1 expression in vascular endothelial cells and promoted angiogenesis [34–36] through exosomes or highly expressed miR-146a [37] and miR21-3p [38] in HUC-MSCs. MSC-Sp significantly increases the secretion of VEGF-α and PDGF-BB in keratinocytes and fibroblasts, which is closely related to neovascularization [39]. Smad is well known as the major inducer of fibroblast differentiation, which is an essential factor for wound healing and downstream mediators of TGFβ1 [40]. In this study, MSC-Sp downregulated TGFβ1, Smad 2/Smad3 expression and upregulated Smad 7 expression of keratinocytes and fibroblasts. MSC-Sp promoted the proliferation and migration of fibroblasts and inhibited the TGFβ1/TGFβ3 ratio and upregulated the TGFβ3, which reduced fibroblast-to-myofibroblast over transformation [41]. Except inhibiting canonical TGFβ/Smad signaling pathway, treatment with MSC-Sp in fibroblasts might influence several non-canonical pathways, including AKT, ERK, RAF, and ROCK to upregulating TGFβ3 [42], but there has been rarely reported. Reduced expression of α-SMA and Col1 in fibroblasts and inhibition of their excessive transformation to TGFβ1-mediated myofibroblasts [43], as well as in vivo HUC-MSCs treatment of diabetic pigs. MiR-21 abundant in MSCs [4], has also been reported to inhibit myofibroblast formation mediated by the TGFβ/Smad2 pathway [44] and promote keratinocyte proliferation and migration by downregulating TGFβ1, tissue inhibitor of metalloproteinase-2 expression, and upregulation of matrix metalloproteinase-9 expression. PL-cultured MSC-Sp promoted keratinocytes expressing VEGF-α, which in turn enhanced the secretion of fibroblasts through HUC-MSCs, and may also inhibit the TGFβ/Smad signaling pathway [43,45].

In vivo experiments, PL + HUC-MSCs treatment significantly promoted DCU healing, collagen formation, and microvascular density in pigs, which was better than HUC-MSCs or PL treatment alone. Moreover, the relative expression of VEGF-α, PDGF-BB, TGFβ1, and α-SMA was higher than that of HUC-MSCs alone, which was similar to the results of MSCs combined with platelet-rich plasma the first-generation platelet product [46–49]. HUC-MSCs treatment alone significantly reduced the expression of α-SMA, Col1, and TGFβ1/TGFβ3 ratio in the process of promoting wound healing. Similar results were observed in the in vivo experiments conducted in this study. This is consistent with observation that MSCs downregulate Col1, α-SMA, and TGFβ1 expression, reduce collagen fiber thickness and scarring[50–52], and upregulate fibroblast and wound TGFβ3 levels to inhibit wound fibrosis [53]. PL + HUC-MSCs and PL alone promoted VEGF-α,TGFβ1, and α-SMA expression similar to platelet-rich plasma [54–56]. Like other platelet rich plasma + MSCs studies, we used pure platelet products, which resulted in the amplification of platelet lysate mechanisms and masking of MSCs to promote wound healing. However, compared to platelet rich plasma, PL is commercially available and stable, which facilitates the translation of basic experiments into clinical trials. Consistent with Liu W et al. [57], HUC-MSCs significantly inhibited the expression of IL-6 during wound healing. Although PL combined with HUC-MSCs increased IL-6, Arg-1 and TGFβ1 expression at the same time, there was no significant difference between the overall IL-6/Arg-1 and IL-6/TGFβ1 ratios among the groups. PL might induce a transient pro-inflammatory response in MSCs during the inflammatory phase of wound healing, subsequently inhibiting the expression of inflammatory factors [58]and resulting in a balance between IL-6/Arg-1 and IL-6/TGFβ1 ratios. However, the inflammatory response during wound healing requires further investigation.

In conclusion, this study found that both HUC-MSCs and PL could promote wound healing, but PL + HUC-MSCs had the best effect compared to treatment alone. PL + HUC-MSCs might regulate wound tissue inflammation by regulating IL-6/Arg-1 and IL-6/

TGFβ1 balance and upregulating wound TGFβ1, VEGF-α, Col1, and α-SMA to promote collagen deposition and wound contraction. This study provides evidence of the clinical use of HUC-MSCs and PL. However, it is necessary to establish PL and HUC- MSCs concentration gradients in animal experiments to determine the optimal concentrations and effects of PL and HUC-MSCs.

Authors contributions

X.W. R, Y.Y.G, and L.H.C conceived the study, executed the animal studies, analyzed, and interpreted the data, and drafted the manuscript. Y. L. and S.Y.S assisted with the animal studies and sample detection. All authors contributed to the manuscript and approved the submitted version.

Ethical approval

The study was approved by the Animal Ethics Committee of the West China Hospital of Sichuan University (No. IACUC 2019232A) since 2019.10.17.

Availability of data and materials

All data supporting the findings of this study are available within the paper and its Supplementary Information.

Statements and declarations funding

Declaration of competing interest

The authors declare that they have no known competing financial interests or personal relationships that could have appeared to influence the work reported in this paper.

Appendix A. Supplementary data

Supplementary data to this article can be found online at https://doi.org/10.1016/j.reth.2024.11.005.

References

[1] Chinese guideline on prevention and management of diabetic foot (2019 edition)(I). 中华糖尿病杂志 2019;(2). 92-93-94-95-96-97-98-99-100-101-102-103-104-105-106-107-108.

[2] Armstrong DG, Swerdlow MA, Armstrong AA, Conte MS, Padula WV, Bus SA. Five year mortality and direct costs of care for people with diabetic foot complications are comparable to cancer. J Foot Ankle Res 2020;13(1):16. https://doi.org/10.1186/s13047-020-00383-2.

[3] Hoffmann A, Floerkemeier T, Melzer C, Hass R. Comparison of in vitro-cultivation of human mesenchymal stroma/stem cells derived from bone marrow and umbilical cord. J Tissue Eng Regen Med 2017;11(9):2565–81. https://doi.org/10.1002/term.2153.

[4] Zhang Y, Pan Y, Liu Y, Li X, Tang L, Duan M, et al. Exosomes derived from human umbilical cord blood mesenchymal stem cells stimulate regenerative wound healing via transforming growth factor-β receptor inhibition. Stem Cell Res Ther 2021;12(1):434. https://doi.org/10.1186/s13287-021-02517-0.

[5] Liu L, Yu Y, Hou Y, Chai J, Duan H, Chu W, et al. Human umbilical cord mesenchymal stem cells transplantation promotes cutaneous wound healing of severe burned rats. PLoS One 2014;9(2):e88348. https://doi.org/10.1371/journal.pone.0088348.

[6] Zhao G, Liu F, Liu Z, Zuo K, Wang B, Zhang Y, et al. MSC-derived exosomes attenuate cell death through suppressing AIF nucleus translocation and enhance cutaneous wound healing. Stem Cell Res Ther 2020;11(1):174. https://doi.org/10.1186/s13287-020-01616-8.

[7] Miranda JP, Filipe E, Fernandes AS, Almeida JM, Martins JP, La Fuente A de, et al. The human umbilical cord tissue-derived MSC population UCX(®) promotes early mitogenic effects on keratinocytes and fibroblasts and G-CSF-mediated mobilization of BM-MSCs when transplanted in vivo. Cell Transplant 2015;24(5):865–77. https://doi.org/10.3727/096368913X676231.

[8] Cheng S, Xi Z, Chen G, Liu K, Ma R, Zhou C. Extracellular vesicle-carried microRNA-27b derived from mesenchymal stem cells accelerates cutaneous wound healing via E3 ubiquitin ligase ITCH. J Cell Mol Med 2020;24(19):11254–71. https://doi.org/10.1111/jcmm.15692.

[9] Fossett E, Khan WS. Optimising human mesenchymal stem cell numbers for clinical application: a literature review. Stem Cell Int 2012;2012:465259. https://doi.org/10.1155/2012/465259.

[10] Mangi AA, Noiseux N, Kong D, He H, Rezvani M, Ingwall JS, et al. Mesenchymal stem cells modified with Akt prevent remodeling and restore performance of infarcted hearts. Nat Med 2003;9(9):1195–201. https://doi.org/10.1038/nm912.

[11] Lee KA, Shim W, Paik MJ, Lee SC, Shin JY, Ahn YH, et al. Analysis of changes in the viability and gene expression profiles of human mesenchymal stromal cells over time. Cytotherapy 2009;11(6):688–97. https://doi.org/10.3109/14653240902974032.

[12] Golchin A, Farahany TZ, Khojasteh A, Soleimanifar F, Ardeshirylajimi A. The clinical trials of mesenchymal stem cell therapy in skin diseases: an update and concise review. Curr Stem Cell Res Ther 2019;14(1):22–33. https://doi.org/10.2174/1574888X13666180913123424.

[13] Wu Y-Y, Jiao Y-P, Xiao L-L, Li M-M, Liu H-W, Li S-H, et al. Experimental study on effects of adipose-derived stem cell-seeded silk fibroin chitosan film on wound healing of a diabetic rat model. Ann Plast Surg 2018;80(5):572–80. https://doi.org/10.1097/SAP.0000000000001355.

[14] Burnouf T, Strunk D, Koh MBC, Schallmoser K. Human platelet lysate: replacing fetal bovine serum as a gold standard for human cell propagation? Biomaterials 2016;76:371–87. https://doi.org/10.1016/j.biomaterials.2015.10.065.

[15] Becherucci V, Piccini L, Casamassima S, Bisin S, Gori V, Gentile F, et al. Human platelet lysate in mesenchymal stromal cell expansion according to a GMP grade protocol: a cell factory experience. Stem Cell Res Ther 2018;9(1):124. https://doi.org/10.1186/s13287-018-0863-8.

[16] Cañas-Arboleda M, Beltrán K, Medina C, Camacho B, Salguero G. Human platelet lysate supports efficient expansion and stability of wharton's jelly mesenchymal stromal cells via active uptake and release of soluble regenerative factors. Int J Mol Sci 2020;21(17). https://doi.org/10.3390/ijms21176284.

[17] Zamani M, Yaghoubi Y, Movassaghpour A, Shakouri K, Mehdizadeh A, Pishgahi A, et al. Novel therapeutic approaches in utilizing platelet lysate in regenerative medicine: are we ready for clinical use? J Cell Physiol 2019;234(10):17172–86. https://doi.org/10.1002/jcp.28496.

[18] Robinson ST, Douglas AM, Chadid T, Kuo K, Rajabalan A, Li H, et al. A novel platelet lysate hydrogel for endothelial cell and mesenchymal stem cell-directed neovascularization. Acta Biomater 2016;36:86–98. https://doi.org/10.1016/j.actbio.2016.03.002.

[19] Protogerou V, Michalopoulos E, Mallis P, Gontika I, Dimou Z, Liakouras C, et al. Administration of adipose derived mesenchymal stem cells and platelet lysate in erectile dysfunction: a single center pilot study. Bioengineering (Basel) 2019;6(1). https://doi.org/10.3390/bioengineering6010021.

[20] Kim S-N, Lee C-J, Nam J, Choi B, Chung E, Song SU. The effects of human bone marrow-derived mesenchymal stem cell conditioned media produced with fetal bovine serum or human platelet lysate on skin rejuvenation characteristics. Int J Stem Cells 2021;14(1):94–102. https://doi.org/10.15283/ijsc20070.

[21] Rhett JM, Ghatnekar GS, Palatinus JA, O'Quinn M, Yost MJ, Gourdie RG. Novel therapies for scar reduction and regenerative healing of skin wounds. Trends Biotechnol 2008;26(4):173–80. https://doi.org/10.1016/j.tibtech.2007.12.007.

[22] Zhang T, Wang X-F, Wang Z-C, Lou D, Fang Q-Q, Hu Y-Y, et al. Current potential therapeutic strategies targeting the TGF-β/Smad signaling pathway to attenuate keloid and hypertrophic scar formation. Biomed Pharmacother 2020;129:110287. https://doi.org/10.1016/j.biopha.2020.110287.

[23] Jiang D, Scharffetter-Kochanek K. Mesenchymal stem cells adaptively respond to environmental cues thereby improving granulation tissue formation and wound healing. Front Cell Dev Biol 2020;8:697. https://doi.org/10.3389/fcell.2020.00697.

[24] Ghosh D, McGrail DJ, Dawson MR. TGF-β1 pretreatment improves the function of mesenchymal stem cells in the wound bed. Front Cell Dev Biol 2017;5:28. https://doi.org/10.3389/fcell.2017.00028.

[25] Shi Y, Wang S, Liu D, Wang Z, Zhu Y, Li J, et al. Exosomal miR-4645-5p from hypoxic bone marrow mesenchymal stem cells facilitates diabetic wound healing by restoring keratinocyte autophagy. Burns Trauma 2024;12:tkad058. https://doi.org/10.1093/burnst/tkad058.

[26] Li L, Zhang J, Zhang Q, Zhang D, Xiang F, Jia J, et al. High glucose suppresses keratinocyte migration through the inhibition of p38 MAPK/autophagy pathway. Front Physiol 2019;10:24. https://doi.org/10.3389/fphys.2019.00024.

[27] Engelgau MM, Thompson TJ, Herman WH, Boyle JP, Aubert RE, Kenny SJ, et al. Comparison of fasting and 2-hour glucose and HbA1c levels for diagnosing

diabetes. Diagnostic criteria and performance revisited. Diabetes Care 1997;20(5):785–91. https://doi.org/10.2337/diacare.20.5.785.

[28] Lazarus GS, Cooper DM, Knighton DR, Percoraro RE, Rodeheaver G, Robson MC. Definitions and guidelines for assessment of wounds and evaluation of healing. Wound Repair Regen 1994;2(3):165–70. https://doi.org/10.1046/j.1524-475X.1994.20305.x.

[29] Suzdaltseva Y, Zhidkih S, Kiselev SL, Stupin V. Locally delivered umbilical cord mesenchymal stromal cells reduce chronic inflammation in long-term nonhealing wounds: a randomized study. Stem Cell Int 2020;2020:5308609. https://doi.org/10.1155/2020/5308609.

[30] Fan D, Zeng M, Xia Q, Wu S, Ye S, Rao J, et al. Efficacy and safety of umbilical cord mesenchymal stem cells in treatment of cesarean section skin scars: a randomized clinical trial. Stem Cell Res Ther 2020;11(1):244. https://doi.org/10.1186/s13287-020-01695-7.

[31] Martinello T, Gomiero C, Perazzi A, Iacopetti I, Gemignani F, DeBenedictis GM, et al. Allogeneic mesenchymal stem cells improve the wound healing process of sheep skin. BMC Vet Res 2018;14(1):202. https://doi.org/10.1186/s12917-018-1527-8.

[32] Nagelschmidt M, Becker D, Bönninghoff N, Engelhardt GH. Effect of fibronectin therapy and fibronectin deficiency on wound healing: a study in rats. J Trauma 1987;27(11):1267–71. https://doi.org/10.1097/00005373-198711000-00011.

[33] Dominici M, Le Blanc K, Mueller I, Slaper-Cortenbach I, Marini F, Krause D, et al. Minimal criteria for defining multipotent mesenchymal stromal cells. The International Society for Cellular Therapy position statement. Cytotherapy 2006;8(4):315–7. https://doi.org/10.1080/14653240600855905.

[34] Seo E, Lim JS, Jun J-B, Choi W, Hong I-S, Jun H-S. Exendin-4 in combination with adipose-derived stem cells promotes angiogenesis and improves diabetic wound healing. J Transl Med 2017;15(1):35. https://doi.org/10.1186/s12967-017-1145-4.

[35] Stefansson S, Lawrence DA. The serpin PAI-1 inhibits cell migration by blocking integrin alpha V beta 3 binding to vitronectin. Nature 1996;383(6599):441–3. https://doi.org/10.1038/383441a0.

[36] Goumans M-J, Lebrin F, Valdimarsdottir G. Controlling the angiogenic switch: a balance between two distinct TGF-b receptor signaling pathways. Trends Cardiovasc Med 2003;13(7):301–7. https://doi.org/10.1016/s1050-1738(03)00142-7.

[37] Ti D, Hao H, Fu X, Han W. Mesenchymal stem cells-derived exosomal microRNAs contribute to wound inflammation. Sci China Life Sci 2016;59(12):1305–12. https://doi.org/10.1007/s11427-016-0240-4.

[38] Hu Y, Rao S-S, Wang Z-X, Cao J, Tan Y-J, Luo J, et al. Exosomes from human umbilical cord blood accelerate cutaneous wound healing through miR-21-3p-mediated promotion of angiogenesis and fibroblast function. Theranostics 2018;8(1):169–84. https://doi.org/10.7150/thno.21234.

[39] Wang L, Wang F, Zhao L, Yang W, Wan X, Yue C, et al. Mesenchymal stem cells coated by the extracellular matrix promote wound healing in diabetic rats. Stem Cell Int 2019;2019:9564869. https://doi.org/10.1155/2019/9564869.

[40] Walraven M, Gouverneur M, Middelkoop E, Beelen RHJ, Ulrich MMW. Altered TGF-β signaling in fetal fibroblasts: what is known about the underlying mechanisms? Wound Repair Regen 2014;22(1):3–13. https://doi.org/10.1111/wrr.12098.

[41] Jiang T, Wang Z, Sun J. Human bone marrow mesenchymal stem cell-derived exosomes stimulate cutaneous wound healing mediates through TGF-β/Smad signaling pathway. Stem Cell Res Ther 2020;11(1):198. https://doi.org/10.1186/s13287-020-01723-6.

[42] Urban L, Čoma M, Lacina L, Szabo P, Sabová J, Urban T, et al. Heterogeneous response to TGF-β1/3 isoforms in fibroblasts of different origins: implications for wound healing and tumorigenesis. Histochem Cell Biol 2023;160(6):541–54. https://doi.org/10.1007/s00418-023-02221-5.

[43] Chellini F, Tani A, Vallone L, Nosi D, Pavan P, Bambi F, et al. Platelet-rich plasma prevents in vitro transforming growth factor-β1-induced fibroblast to myofibroblast transition: involvement of vascular endothelial growth factor (VEGF)-A/VEGF receptor-1-mediated signaling (†). Cells 2018;7(9). https://doi.org/10.3390/cells7090142.

[44] Fang S, Xu C, Zhang Y, Xue C, Yang C, Bi H, et al. Umbilical cord-derived mesenchymal stem cell-derived exosomal MicroRNAs suppress myofibroblast differentiation by inhibiting the transforming growth factor-β/SMAD2 pathway during wound healing. Stem Cells Transl Med 2016;5(10):1425–39. https://doi.org/10.5966/sctm.2015-0367.

[45] Sassoli C, Pini A, Chellini F, Mazzanti B, Nistri S, Nosi D, et al. Bone marrow mesenchymal stromal cells stimulate skeletal myoblast proliferation through the paracrine release of VEGF. PLoS One 2012;7(7):e37512. https://doi.org/10.1371/journal.pone.0037512.

[46] Liu Z, Xiao S, Tao K, Li H, Jin W, Wei Z, et al. Synergistic effects of human platelet-rich plasma combined with adipose-derived stem cells on healing in a mouse pressure injury model. Stem Cell Int 2019;2019:3091619. https://doi.org/10.1155/2019/3091619.

[47] Hadad I, Johnstone BH, Brabham JG, Blanton MW, Rogers PI, Fellers C, et al. Development of a porcine delayed wound-healing model and its use in testing a novel cell-based therapy. Int J Radiat Oncol Biol Phys 2010;78(3):888–96. https://doi.org/10.1016/j.ijrobp.2010.05.002.

[48] Hosni Ahmed H, Rashed LA, Mahfouz S, Elsayed Hussein R, Alkaffas M, Mostafa S, et al. Can mesenchymal stem cells pretreated with platelet-rich plasma modulate tissue remodeling in a rat with burned skin? Biochem Cell Biol 2017;95(5):537–48. https://doi.org/10.1139/bcb-2016-0224.

[49] Myung H, Jang H, Myung JK, Lee C, Lee J, Kang J, et al. Platelet-rich plasma improves the therapeutic efficacy of mesenchymal stem cells by enhancing their secretion of angiogenic factors in a combined radiation and wound injury model. Exp Dermatol 2020;29(2):158–67. https://doi.org/10.1111/exd.14042.

[50] Li M, Luan F, Zhao Y, Hao H, Liu J, Dong L, et al. Mesenchymal stem cell-conditioned medium accelerates wound healing with fewer scars. Int Wound J 2017;14(1):64–73. https://doi.org/10.1111/iwj.12551.

[51] Huang S, Wu Y, Gao D, Fu X. Paracrine action of mesenchymal stromal cells delivered by microspheres contributes to cutaneous wound healing and prevents scar formation in mice. Cytotherapy 2015;17(7):922–31. https://doi.org/10.1016/j.jcyt.2015.03.690.

[52] Millán-Rivero JE, Martínez CM, Romecín PA, Aznar-Cervantes SD, Carpes-Ruiz M, Cenis JL, et al. Silk fibroin scaffolds seeded with Wharton's jelly mesenchymal stem cells enhance re-epithelialization and reduce formation of scar tissue after cutaneous wound healing. Stem Cell Res Ther 2019;10(1):126. https://doi.org/10.1186/s13287-019-1229-6.

[53] Wu Y, Peng Y, Gao D, Feng C, Yuan X, Li H, et al. Mesenchymal stem cells suppress fibroblast proliferation and reduce skin fibrosis through a TGF-β3-dependent activation. Int J Low Extrem Wounds 2015;14(1):50–62. https://doi.org/10.1177/1534734614568373.

[54] Ren Z-Q, Du B, Dong H-J, Duan G-H, Du A-C, Wang Y, et al. Autologous platelet-rich plasma repairs burn wound and reduces burn pain in rats. J Burn Care Res 2022;43(1):263–8. https://doi.org/10.1093/jbcr/irab079.

[55] Wei S, Xu P, Yao Z, Cui X, Lei X, Li L, et al. A composite hydrogel with co-delivery of antimicrobial peptides and platelet-rich plasma to enhance healing of infected wounds in diabetes. Acta Biomater 2021;124:205–18. https://doi.org/10.1016/j.actbio.2021.01.046.

[56] Zhou M, Lin F, Li W, Shi L, Li Y, Shan G. Development of nanosilver doped carboxymethyl chitosan-polyamideamine alginate composite dressing for wound treatment. Int J Biol Macromol 2021;166:1335–51. https://doi.org/10.1016/j.ijbiomac.2020.11.014.

[57] Liu W, Yu M, Xie D, Wang L, Ye C, Zhu Q, et al. Melatonin-stimulated MSC-derived exosomes improve diabetic wound healing through regulating macrophage M1 and M2 polarization by targeting the PTEN/AKT pathway. Stem Cell Res Ther 2020;11(1):259. https://doi.org/10.1186/s13287-020-01756-x.

[58] Romaldini A, Mastrogiacomo M, Cancedda R, Descalzi F. Platelet lysate activates human subcutaneous adipose tissue cells by promoting cell proliferation and their paracrine activity toward epidermal keratinocytes. Front Bioeng Biotechnol 2018;6:203. https://doi.org/10.3389/fbioe.2018.00203.